Ellipsometry Studies of the Self-Assembly of Nonionic Surfactants at the Silica–Water Interface: Equilibrium Aspects

Fredrik Tiberg,* Bengt Jönsson, Ji-an Tang,† and Björn Lindman

Physical Chemistry 1, Chemical Centre, Lund University, P. O. Box 124, S-221 00 Lund, Sweden

Received October 6, 1993. In Final Form: April 5, 1994®

The nature of layers of a series of poly(ethylene glycol) monoalkyl ethers (C_nE_m) adsorbed on silica surfaces has been systematically investigated by means of null ellipsometry. The results show that adsorption remains low until a well-defined concentration ((≈0.6–0.9)cmc) is exceeded. Then, as surfactants in the interfacial region start to self-assemble, it increases abruptly and plateau adsorption is generally observed prior to the cmc. The normal extension of the interfacial aggregates is relatively constant from intermediate to high surface coverage. Increasing the ethylene oxide to hydrocarbon ratio results in a decreased adsorption. The mean optical thickness, on the other hand, is relatively independent of the number of ethylene oxide groups in the surfactant but almost linearly dependent on the length of the hydrocarbon tail. The values obtained for these parameters suggest that the adsorbed layer is built up of discrete surface aggregates, or micelles, with dimensions resembling those observed in bulk solution. A more refined optical model of the adsorbed layer confirms the notion of surface micelles growing with increasing hydrocarbon content. It also points out that the extension of the surface micelles is slightly larger than the measured mean optical thickness. In addition to studies of neat C_nE_m surfactants, we also examine the adsorption of mixed surfactant systems. Changes observed in adsorption on altering the bulk ratio of two surfactants are well correlated to the bulk micellar surfactant ratio calculated by ideal solution theory.

Introduction

Adsorption of nonionic surfactants is, as a consequence of their practical importance and rich bulk and interfacial behavior, a field subject to high research activity (cf. reviews 1–3). It is suggested that surfactants often associate into interfacial aggregates when adsorbed onto hydrophilic surfaces, such as silica.[4–8] The size and shape of these aggregates are, for nonionic surfactants, most likely controlled by the relative sizes of the head groups and the tails of the surfactants. Thus, depending on surfactant composition, these aggregates might be discrete and enclose a finite region or be continuous and form bilayers. A systematic experimental study of the effect of the surfactant composition on the adsorbed layer properties is, however, still lacking.

In an attempt do this, we recently developed a simple and rather accurate procedure for in situ characterization of thin films (<100 Å) by means of null ellipsometry.[8] By this approach the properties of the adsorbed film are determined by first measuring the substrate in different ambient media, possessing different refractive indices, and then using this data to apply the appropriate optical model for the interpretation of the adsorption data. In the case of poly(ethylene glycol) alkyl ether films adsorbed at the silica–water interface, the methodology enables time-resolved, and relatively accurate, separate determinations of mean optical layer thicknesses and refractive indices in addition to the usual data on the adsorbed amount. For $C_{12}E_5$ and $C_{12}E_6$, these measurements were found to be in good agreement with those obtained by other methods, namely X-ray and neutron scattering,[5,8–10] neutron reflection,[6,7] and hydrodynamic techniques.[7]

In addition to the effects of surfactant molecular structure and composition on the nature of the adsorbed layers of single surfactants, we also investigate the effects of mixing. The latter issue is of great scientific interest, but also of considerable technical relevance, since commercial surfactants are often rather polydisperse. A presentation of dynamic aspects associated with the adsorption of these substances is to be presented separately.

Experimental Section

Method and Equipment. The adsorption is studied by means of *in situ* null ellipsometry.[11] The instrument used in this study was an automated Rudolph Research thin-film ellipsometer, Type 43603-200E, equipped with high-precision stepper motors and controlled by a personal computer. All measurements were performed at the wavelength $\lambda = 4015$ Å and the angle of incidence $\phi = 67.2°$. The experimental set-up, as well as the procedure for in situ characterization of thin films adsorbed on layered substrates, has been presented previously.[8]

In brief, to obtain reliable measures of thickness and refractive index of an adsorbed surfactant film, the optical characteristics of the oxidized silicon wafer must first be properly determined. At the beginning of each experiment, the optical properties of the Si/SiO_2 substrate were determined by ellipsometric mea-

† On leave from the Institute of Photographic Chemistry, Academica Sinica, P. O. Box 772, Beishatan, Dewai, Beijing 100 101, China.

® Abstract published in *Advance ACS Abstracts,* June 15, 1994.

(1) Clunie, J. S.; Ingram, B. T. In *Adsorption from Solution at the Solid/Liquid Interface*; Parfitt, G. D., Rochester, C. H., Eds.; Academic Press: New York, 1983; pp 105–152.
(2) von Rybinsky, W.; Schwuger, M. J. In *Surfactant Science Series*; Schick, M. J., Ed.; Marcel Dekker: New York, 1987; Vol. 23.
(3) Cases, J. M.; Villieras, F. *Langmuir* **1992**, *8*, 1251.
(4) Levitz, P.; Van Damme, H.; Keravis, D. *J. Phys. Chem.* **1984**, *88*, 2228.
(5) Cummins, P. G.; Staples, E.; Penfold, J. *J. Phys. Chem.* **1990**, *94*, 3740.
(6) McDermott, D. C.; Lu, J. R.; Lee, E. M.; Thomas, R. K.; Rennie, A. R. *Langmuir* **1992**, *8*, 1204.
(7) Böhmer, M. R.; Koopal, L. K.; Janssen, R.; Lee, E. M.; Thomas, R. K.; Rennie, A. R. *Langmuir* **1992**, *8*, 2228.
(8) Tiberg, F.; Landgren, M. *Langmuir* **1993**, *9*, 927.
(9) Cummins, P. G.; Penfold, J.; Staples, E. *J. Phys. Chem.* **1992**, *96*, 8092.
(10) Gellan, A.; Rochester, C. H. *J. Chem. Soc., Faraday Trans. 1* **1985**, *81*, 2235.
(11) Azzam, R. M. A.; Bashara, N. M. *Ellipsometry and Polarized Light*; North Holland: Amsterdam, 1989.

0743-7463/94/2410-2294$04.50/0

Table 1. Refractive Index Increment (dn/dc), Critical Micellar Concentration (cmc), Critical Surface Aggregation Concentration (csac), Adsorbed Amount (Γ), Apparent Surface Area per Surfactant Molecule (σ), Mean Adsorbed Layer Thickness (d_f), and Maximal Axial Ratio of Adsorbed Aggregates (ϱ) (The Subscript p Denotes Plateau Values)

surfactant	dn/dc[30]	cmc[31] (mmol·L^{-1})	csac (mmol·L^{-1})	Γ_p (μmol·m^{-2})	σ (Å^{-2})	$d_{f,p}$ (Å)	ϱ_{max}
$C_{10}E_6$	0.129	0.90	0.70	2.5	66	36	4
$C_{12}E_5$	0.131	0.057	0.050	5.7	29	42	19
$C_{12}E_6$	0.136	0.087	0.065	4.1	40	41	13
$C_{12}E_8$	0.142	0.092	0.060	1.8	92	44	3
$C_{14}E_6$	0.135	0.010	0.0060	5.2	32	47	24
$C_{16}E_6$	0.133	0.0017	0.0012	5.4	30	52	26

surements in air and then in water, as in ref 8. After the measurements of the bare substrate were accomplished, a controlled amount of surfactant was added into the thermostated cuvette, originally containing 5 mL of H_2O. The ellipsometrical angles ψ and Δ were then monitored as a function of time until steady-state adsorption was ascertained. All measurements were performed at a temperature of 25 ± 0.1 °C under continuous stirring by a magnetic stirrer at about 300 rpm.

From the measured values of ψ and Δ, the mean optical thickness (d_f) and the refractive index (n_f) were calculated according to a numerical procedure described earlier,[8] using an optical four-layer model of the silicon–silica-adsorbed layer-ambient system. The variables n_f and d_f were then used to calculate the adsorbed mass (Γ) according to de Feijter's formula[12]

$$\Gamma = \frac{(n_f - n_o)d_f}{\frac{dn}{dc}} \quad (1)$$

where the refractive index increment (dn/dc) values used are listed in Table 1 and n_0 is the refractive index of the ambient bulk solution. The results presented in this paper are the outcome of at least two adsorption runs during which a minimum of 50 measurements were performed. These are collected during approximately 0.5 h after steady-state conditions have been recognized. The errors in d_f, n_f, and Γ presented here were estimated to ±5 Å, ±0.006 and ±0.2 μmol·m^{-2}, respectively.

Materials. A series of monodisperse poly(oxyethylene glycol) alkyl ethers (C_nE_m; $C_{10}E_6$, $C_{12}E_5$, $C_{12}E_6$, $C_{12}E_8$, $C_{14}E_6$, and $C_{16}E_6$) were purchased from Nikko Chemicals and used without further purification. The reason for choosing these surfactants is that they are very well characterized and have suitable compositions and cmc's for our purpose. Important properties of these surfactants are presented in Table 1. These surfactants further display interesting properties on hydrophilic interfaces, and the inhomogeneity with respect to the refractive index of the surfactant layer is relatively small compared to that of many other surfactant systems.

Polished silicon test slides (p-type, boron doped, resistivity 1–20 Ω-cm) were purchased from Okmetic Ltd. The wafers were oxidized thermally in pure saturated oxygen at 920 °C for ≈1 h followed by annealing and cooling in argon flow. This procedure resulted in a SiO_2 layer thickness of ≈300 Å. The oxidized wafers were then cut into slides with a width of 12.5 mm. Cleaning was performed in a mixture of 25% NH_4OH (pro Analysi, Merck), 30% H_2O_2 (pro analysi, Merck), and H_2O (1:1:5, by volume) at 80 °C for 5 min, followed by cleaning in a mixture of 32% HCl (pro analysi, Merck), 30% H_2O_2 (pro analysi, Merck), and H_2O (1:1:5, by volume) at 80 °C for 5 min. Then the slides were rinsed twice, first in distilled water and then in ethanol. They were then kept in absolute ethanol until use. Just before the slides were placed in the ellipsometer cuvette, they were treated in a plasma cleaner (Harrick Scientific Corporation, Model PDC-3XG) for 5 min. The plasma treatment was performed with residual argon (0.1 mbar) at a power of 30 W.

Results

Isotherms for different poly(ethylene glycol) monoalkyl ethers (C_nE_m) with varying size of the polar head groups (n = 12; m = 5, 6, and 8) are shown in Figure 1, while those for surfactants with different hydrocarbon tail sizes (n = 10, 12, 14, 16; m = 6) are displayed in Figure 2.

(12) de Feijter, J. A.; Benjamins, J.; Veer, F. A. *Biopolymers* **1978**, *17*, 1759.

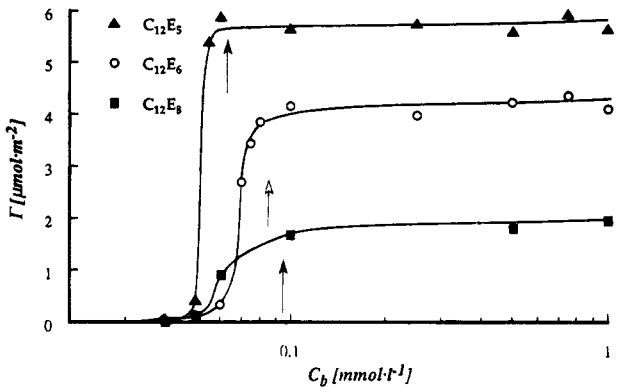

Figure 1. Adsorption isotherms for three different poly(ethylene glycol) monododecyl ethers at T = 25 °C. The cmc's of the different surfactants are indicated with open and filled arrows, respectively. Note that the bulk concentration of surfactant (C_b) is presented on a logarithmic scale. Solid lines are only drawn to guide the eye.

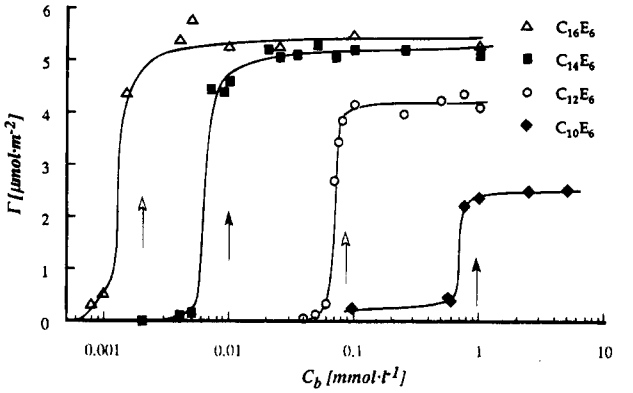

Figure 2. Adsorption isotherms for three different hexa(ethylene glycol) monoalkyl ethers at T = 25 °C. The cmc's for the different surfactants are indicated with open and filled arrows, respectively. Note that the bulk concentration of surfactant (C_b) is presented on a logarithmic scale. Solid lines are only drawn to guide the eye.

Adsorption remains low for all surfactants until a concentration of about (0.6–0.9)cmc is reached. Increasing the concentration above this value results in a strong increase of the adsorption followed by a stable plateau. Note that the increase is close to steplike for surfactants with a low content of hydrophilic ethylene oxide (EO) groups. For surfactants with higher EO content, the cooperativity largely disappears and is replaced by a more gradual transition from low to high surface coverage. Plateau adsorption is, however, reached prior to the cmc for all surfactants studied in this investigation. Another feature worth observing is the fact that the adsorption prior to the sharp rise is higher for the decyl surfactant than for those with longer hydrocarbon tails. The trends in the adsorbed amount with varying concentration are also observed when the mean refractive index (n_f) of the adsorbed film is plotted against the concentration (see ref 8).

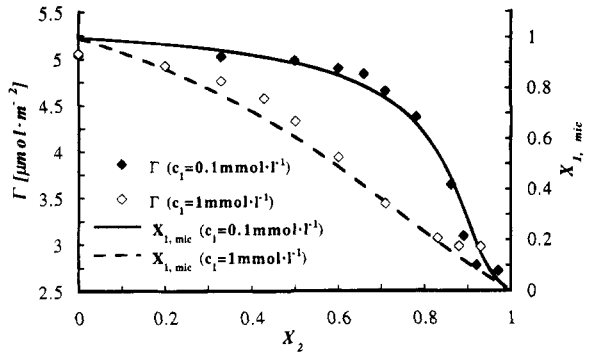

Figure 3. Adsorbed amount (Γ) and the fraction of $C_{14}E_6$ in the mixed micelles ($X_{1,mic}$, given by eq 3 and 4) at two different constant bulk concentrations (c_1) of $C_{14}E_6$ as a function of the total fraction of $C_{10}E_6$ in the solution (X_2).

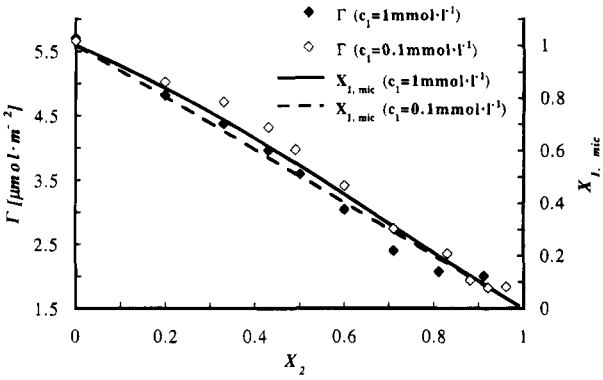

Figure 4. Adsorbed amount (Γ) and the fraction of $C_{12}E_5$ in the mixed micelles ($X_{1,mic}$, given by eq 3 and 4) at two different constant bulk concentrations (c_1) of $C_{12}E_5$ as a function of the total fraction of $C_{12}E_8$ in the solution (X_2).

The effects of mixing two monodisperse surfactant samples were also investigated, and the results are presented in Figures 3 and 4, where the total adsorption of pure surfactants and mixtures thereof is plotted against the composition. The measurements were performed at two different total concentrations (0.1 and 1 mmol·L^{-1}) of $C_{14}E_6$ and $C_{12}E_5$ and varying amounts of $C_{10}E_6$ and $C_{12}E_8$, respectively. In the $C_{14}E_6/C_{10}E_6$ case shown in Figure 3 we have cmc's that differ by 2 orders of magnitude, while in the $C_{12}E_5/C_{12}E_8$ system displayed in Figure 4 the cmc's are of the same order of magnitude. For consistency, the adsorbed amount is presented as μmol·m^{-2}. The average molecular weights used for the conversion from mg to μmol were obtained by assuming that the composition in the adsorbed layer varies linearly with the adsorbed amount. This may not be absolutely correct, but errors associated with this assumption are not significant. It is obvious from the figures that the additions of a surfactant with higher EO/C ratio result in a decrease of the adsorbed amount. The path from one single surfactant system to another depends on the relations between the total concentration and the cmc's of the surfactants. In contrast, no effect on the adsorbed amounts was observed upon additions of a small poly(ethylene oxide) oligomer (MW = 600). Additions of a larger poly(ethylene oxide) (MW = 6000) result, however, in a total replacement of all surfactants studied with polymers at the interface.

The mean optical thickness (d_f) for $C_{12}E_5$, $C_{12}E_6$, and $C_{12}E_8$ versus the bulk surfactant concentration (C_b) is presented in Figure 5. It is clear from this graph that the mean optical thickness varies in a manner similar to that of the adsorbed amount, although the increase in d_f also appears sharp for the surfacants with rather large EO head groups.

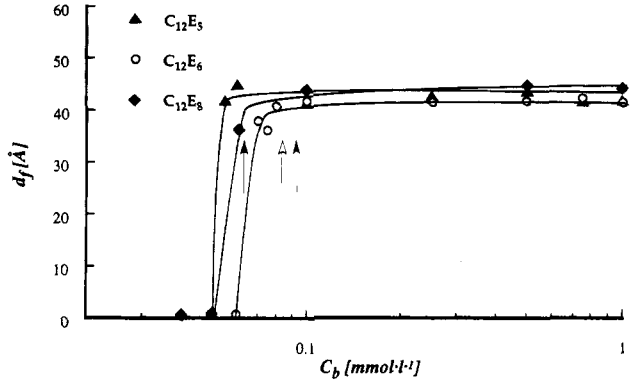

Figure 5. Mean optical thickness (d_f) of adsorbed poly(ethylene glycol) monododecyl ethers versus bulk concentration (C_b) at $T = 25$ °C. The cmc's of the different surfactants are indicated with open and filled arrows. Solid lines are only drawn to guide the eye.

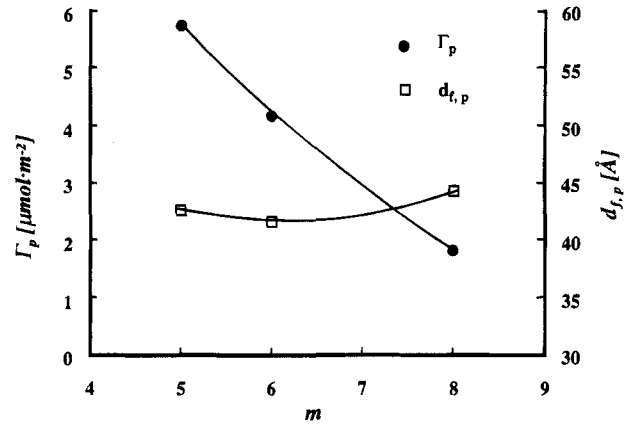

Figure 6. Plateau adsorption (Γ_p) and mean optical thickness ($d_{f,p}$) as a function of the number of ethylene oxide (m) groups in the ethylene oxide head group for polyethylene glycol monododecyl ethers. Solid lines are only drawn to guide the eye.

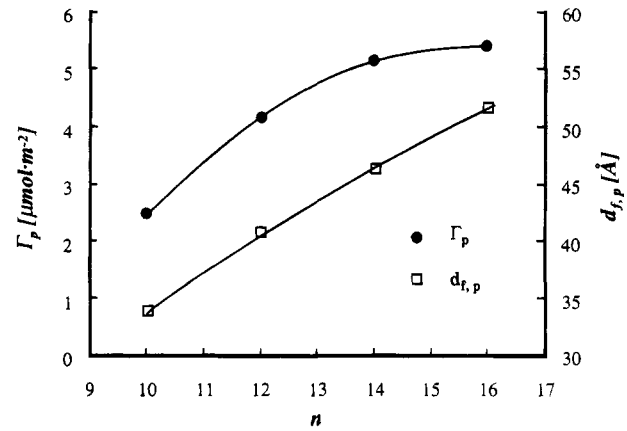

Figure 7. Plateau adsorption (Γ_p) and plateau mean optical thickness ($d_{f,p}$) as a function of the number of carbons (n) in the hydrocarbon tail for hexa(ethylene glycol) monoalkyl ethers. Solid lines are only drawn to guide the eye.

Average plateau values of the adsorbed amount (Γ_p) and the mean optical thickness ($d_{f,p}$) for dodecyl surfactants are plotted as a function of the number of ethoxy groups (m) in the head group in Figure 6. Corresponding data for hexa(ethylene glycol) surfactants with varying number of carbons (n) in the hydrocarbon tail are shown in Figure 7. The adsorbed amount increases with increasing carbon or decreasing ethoxy number. For the hexa(ethylene glycol) series it is further seen that this increase levels off at $n \approx 14$. The thickness, on the other hand, displays a

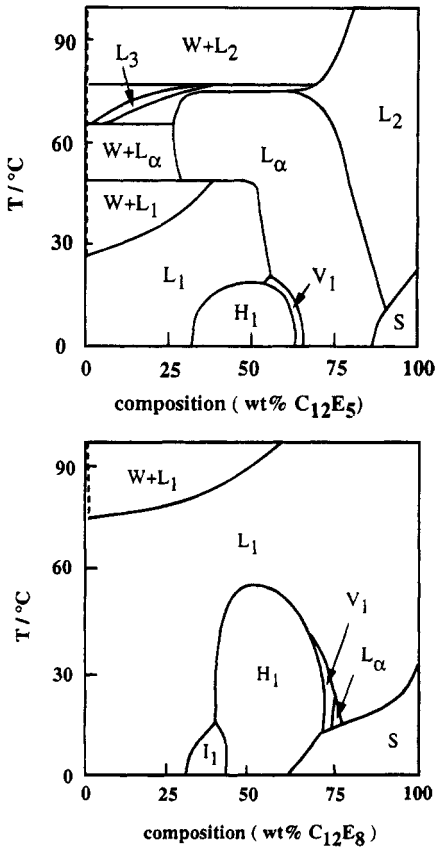

Figure 8. Schematic experimental phase diagrams of the $C_{12}E_5$/water (upper graph) and $C_{12}E_8$/water (lower graph) systems over the temperature range 0–100 °C. The diagrams are redrawn from ref 15. L_1, L_2, L_3 and W are isotropic solution phases, I_1 cubic phase of packed spherical micelles, V_1 normal bicontinuous cubic phase, H_1 normal hexagonal phase, L_α lamellar phase, and S the solid surfactant.

rather different behavior. Thus, varying the number of EO groups (m) does not result in any significant change of the observed plateau thickness. An increase in the size of the hydrocarbon tail, however, results in a close to linear increase of the mean thickness of the adsorbed film with a number of carbons in the chain.

Discussion

The most significant feature of surfactant molecules in water (and some other polar solvents) is their self-assembly. This leads to aggregates of a wide range of geometries, from spherical micelles to bilayers and reversed-type structures. The best information on the polymorphism of the aggregates is provided by the phase behavior. A large number of different phases have been identified for surfactant–water systems, and the main molecular features controlling the relative stability of the most common phases have begun to become well understood.[13,14] For the nonionic surfactants studied in this work, the typical sequence with increasing surfactant concentration: spherical micelles–rod micelles (or cubic liquid crystal)–hexagonal 1 c–cubic 1 c–lamellar 1 c–reversed micellar, is obtained, but for a given surfactant at a given temperature only a few of the phases appear.[15] As indicated in the phase diagrams shown in Figure 8, $C_{12}E_5$ shows a wide stability range for the lamellar phase, while for $C_{12}E_8$ this phase has almost disappeared and has been replaced by micellar and hexagonal regions that now extend over a large portion of the phase diagram. With increasing temperature and concentration, $C_{12}E_5$ micelles show a tendency to grow, and there may be a transition from micellar phase to lamellar liquid crystal. $C_{12}E_8$ micelles, on the other hand, remain small and roughly spherical even at higher temperatures and concentrations.[16] These observations are prevalent for this class of surfactants and consistent with changes of the head group area and hydrophilic portion of the surfactant.

The self-assembly is also influenced by different cosolutes. Many of these lower the free energy of association and consequently reduce the cmc and/or promote aggregate growth. Macromolecular cosolutes in particular may significantly shift the cmc, due to various effects that contribute to the favored self-assembly at a polymer chain. Macroscopic interfaces may also influence surfactant self-assembly, and the interaction energy per surfactant molecule can, both in this case and in that of polymer chains, be very low in spite of major effects, due to the large aggregation numbers.

In the present study we have considered a series of nonionic surfactant molecules at the silica–water interface. Because of the high precision of the ellipsometer used, minute changes in adsorption as a function of surfactant chemical structure can be ascertained. All measured adsorption isotherms (Figures 1 and 2) display a high degree of cooperative behavior and demonstrate that surfactant–interface interactions are best described in terms of surface induced, or facilitated, self-assembly. The interaction between the surface and surfactant unimers is clearly very small, although we can identify a small contribution, ranging from 0 to about 0.4 μmol·m^{-2} in the concentration region prior to the sharp rise in adsorption. The high values are notably observed for $C_{10}E_6$ in a concentration region where the ethylene oxide oligomers have been shown to reach maximum adsorption.[17]

The sharp rise in adsorption observed prior to the cmc indicates that lateral interactions between surfactant unimers start to come into play. It has, indeed, been shown experimentally by fluorescence spectroscopy measurements by Levitz et al.[4,18] that these interactions result in the formation of interfacial aggregates just prior to the cmc. The break point where the self-assembly related increase in adsorption is first noticed is rather well defined ((0.6–0.9)cmc, Table 1) and will hereafter be referred to as the critical surface aggregation concentration (csac). We note that the difference between the two parameters is quite small, thus confirming that the interaction between the surface and the surfactant molecules is quite weak, <0.5 kT. As the bulk surfactant concentration attains the cmc value, the surfactant activity reaches its maximum value to good approximation, and therefore, no further adsorption takes place as the concentration is increased. This implies that the adsorption process occurs mainly below the cmc, in agreement with the conclusion drawn earlier from equilibrium and kinetic studies by Klimenko and co-workers,[19] although the experimental results in that investigation differ in important aspects from those obtained by us.[20]

(13) Jönsson, B.; Wennerström, H. *J. Colloid Interface Sci.* **1981**, *80*, 482.
(14) Israelachvili, J. *Intermolecular & Surface Forces*, 2nd ed.; Academic Press Limited: London, 1991.
(15) Mitchell, J. D.; Tiddy, G. J. T.; Waring, L.; Bostock, T.; McDonald, M. P. *J. Chem. Soc., Faraday Trans. 1* **1983**, *79*, 975.
(16) Nilsson, P. G.; Wennerström, H.; Lindman, B. *J. Phys. Chem.* **1983**, *87*, 1377.
(17) Trens, P.; Denoyel, R. *Langmuir* **1993**, *9*, 519.
(18) Levitz, P.; Van Damme, H. *J. Phys. Chem.* **1986**, *90*, 1302.
(19) Klimenko, N. A.; Permilovsaya, A. A.; Traysorukova, A. A.; Kaganovskii, A. M. *Kolloidnyi Z.* **1975**, *37*, 972.
(20) Tiberg, F.; Jönsson, B.; Lindman, B. *Langmuir*, submitted.

The location of the break point, the general shape of the isotherm and the magnitude of the plateau adsorption agree rather well with theoretical predictions,[21,22] as well as with experimental findings on similar surfactant systems.[4-10,22] Some ambiguity regarding the location of the breakpoint where the large increase in adsorption is first observed does, however, exist between different studies. This might, as we stated previously, be due to the extremely slow kinetics observed in this region, but it could also be an effect of different surface properties and/or polydispersity of the surfactant sample.[8] A crossover point at low coverage is also observed between the $C_{12}E_6$ and $C_{12}E_8$ isotherms. This has been shown earlier for $C_{12}E_6$ and $C_{12}E_{25}$ by Böhmer et al.,[7] who further demonstrated this finding for systems in which the head group adsorbs at the interface, by means of self-consistent field theory. The observation that the csac is shifted to lower concentrations, relative to the cmc, for surfactants with longer EO chains indicates that the adsorption energy per surfactant molecule increases with increasing EO chain length. The striking similarity in the isotherm and the plateau surfactant adsorption, observed for surfactants with similar EO/C ratio, shows, however, that monomer–monomer surfactant interactions are of primary importance to the adsorption and that variation in head group/surface interactions due to variation of head group size plays a minor role.

From the adsorbed amounts we obtain an apparent surface area per surfactant molecule (the σ value in Table 1). If we assume that the adsorbed surfactants form complete bilayers at the surface, then the area per head group is twice this value, i.e., 58 and 184 Å^2 for $C_{12}E_5$ and $C_{12}E_8$, respectively. The head group area of $C_{12}E_5$ in the lamellar 1 c phase is about 45 Å^2.[23] Thus, in the case of $C_{12}E_5$, the surface self-assembly results in the formation of aggregates that may or may not be discrete, while the much larger value for $C_{12}E_8$ is only compatible with a discrete structure, like micelles, at the interface. It is not possible to probe the interfacial structure from the values of the adsorbed amount, but we note that the general trends agree well with that observed in bulk solution.

In order to compare the association behavior in bulk solution with that at the solid–liquid interface and to relate mono- and polydisperse systems we further performed a series of measurements where the adsorption of mixtures of monodisperse surfactants was studied. The adsorption in the presence of micelles can be viewed as a competition between surface aggregates and bulk micelles of surfactant. The adsorption data on the mixed systems is presented together with calculated mixed micellar properties to see whether the composition of the mixed surface aggregates, due to specific surfactant interactions in the aggregates or with the surface, differ from that of the bulk micelles. To calculate the micelle composition, we used ideal solution theory,[24] which has been shown to apply to nonionic systems. This theory gives the following expression for the concentration of the individual components in the micelles

$$c_{1,\mathrm{mic}} = c_1 - \frac{-(c-\delta) + \sqrt{(c-\delta)^2 + 4c_1\delta}}{2\left(\frac{\mathrm{cmc}_2}{\mathrm{cmc}_1} - 1\right)} \qquad (2)$$

where 1 and 2 represent either $C_{14}E_6$ or $C_{12}E_5$ and $C_{10}E_6$ or $C_{12}E_8$, respectively. c is the total surfactant concentration ($c_1 + c_2$), and $\delta = \mathrm{cmc}_1 - \mathrm{cmc}_2$. The fraction of the surfactants ($C_{14}E_6$ or $C_{12}E_5$) in the mixed micelles is then obtained as

$$X_{1,\mathrm{mic}} = \frac{c_{1,\mathrm{mic}}}{c_{1,\mathrm{mic}} + c_{2,\mathrm{mic}}} \qquad (3)$$

and plotted against the bulk ratio of $C_{10}E_6$ and $C_{12}E_8$ in Figures 3 and 4, respectively. It is clear from these figures that there are strong correlations between, on the one hand, the compositions of the mixed micelles and the adsorption, and thus the composition of the interfacial aggregates, on the other. The shape of the adsorption curves deviates slightly from the theoretical predictions of the bulk micellar composition. The sigmoidal shape of the adsorption versus bulk ratio curves may indicate the presence of small steric constraints, which to some extent seem to prevent ideal mixing in the surface aggregates at low and high bulk ratios. This could be due to the fact that surface micelles have a more planar structure, since the adsorbed layer thickness of the $C_{14}E_6/C_{10}E_6$ system is likely to be controlled by the surfactant with the highest ratio in the aggregate. Incorporating a decyl chain when the aggregates are dominated by tetradecyl chains, or vice versa, will then lead to exposure of some of the chains to a less hydrophobic environment. This picture was proposed by Roberts et al.[25] who observed a similar phenomenon for mixed anionic surfactants adsorbed on alumina. The effect is, however, very small, and the size of the surfactant aggregates, whether located in the vicinity of the surface or in the solution, is likely to have a similar dependence on the surfactant ratio.

The fact that the mean optical thickness and the mean refractive index of the film can be calculated separately contributes further to a unique understanding of the structure of the adsorbed layer. From Figure 5 it is clear that the plateau thickness is obtained directly by increasing the concentration above the csac. This shows that there is no formation at first of other intermediate aggregates, such as hemimicelles or monolayers, at the surface. The subsequent increase in adsorption observed for $C_{12}E_6$ and $C_{12}E_8$ after the plateau thickness has been established is instead the result of a more effective packing of the surface aggregates at the surface and/or simply a two-dimensional growth of these in the surface plane. An analogous finding is observed in the dynamics of adsorption,[20] where d_f changes very little in the interval ranging from intermediate to high coverage. The feature is seen during both adsorption and desorption.

In Figure 5 and 6, it can also be seen that the plateau thickness remains more or less constant when the number of hydrophilic EO groups (m) of dodecyl surfactants is varied from five to eight. The adsorbed amount on the other hand decreases by roughly a factor of 3 when $C_{12}E_5$ is replaced by $C_{12}E_8$. This indicates that $C_{12}E_8$ forms small discrete aggregates at the interface, whereas $C_{12}E_5$ forms more extended structures, like oblates or bilayers. The observation that the extension of the aggregates normal to the surface is rather insensitive to the number of EO groups in the head group is also observed in the lamellar liquid crystalline phase.[26] As the molecular volume of the surfactant increases, due to added EO groups, the

(21) Böhmer, M. R.; Koopal, L. K. *Langmuir* **1990**, *6*, 1478.
(22) Levitz, P. *Langmuir* **1992**, *7*, 1595.
(23) Strey, R.; Schomäcker, R.; Roux, D.; Nallet, F.; Olsson, U. *J. Chem. Soc., Faraday Trans.* **1990**, *86*, 2253.
(24) Clint, J. H. *J. Chem. Soc., Faraday Trans. 1* **1975**, *71*, 1327.
(25) Roberts, B. L.; Scamehorn, J. F.; Harwell, J. H. In *Phenomena in Mixed Surfactant Systems*; Scamehorn, J. F., Ed.; American Chemical Society: Washington, DC, 1987.
(26) Carvell, M.; Denver, D. G.; Lyle, I. G.; Tiddy, G. J. T. *Faraday Discuss. Chem. Soc.* **1986**, *81*, 223.

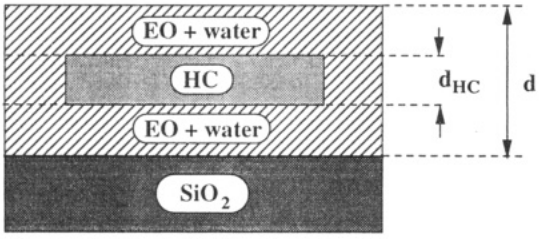

Figure 9. Sketch of the optical model of the adsorbed layer used for the calculations of the hydrocarbon layer thickness (d_{HC}) and the total layer thickness (d) presented in Figures 10–12. The adsorbed layer is modelled as consisting of an interior HC + EO–water part surrounded by an EO–water layer.

head-group area increases likewise and the bilayer thickness remains nearly constant. While varying the length of the EO chain gives insignificant changes to the mean optical thickness (Figure 6), varying the alkyl chain length results in a major change (Figure 7). The increase in the thickness of the surfactant layer is close to linear with the number of carbons (n) in the alkyl chain. The increment for one monomer is 1–1.5 Å per carbon. This is in agreement with the increment in length of a fully extended hydrocarbon chain (=1.27 Å),[27] which normally governs the dimensions of surfactant self-assemblies for bulk phases.

Both the magnitude of the mean optical layer thickness and the fact that this does not change with the size of the polar tail are in good accord with data obtained by means of X-ray and neutron scattering measurements[5,9,10] as well as with hydrodynamic data.[7] The value of the thickness is, however, slightly smaller than that obtained by neutron reflection measurements.[6,7]

The mean optical thickness (d_f) and the refractive index (n_f) discussed so far represent an equivalent real adsorbed layer thickness in the case where we have a uniform refractive index throughout the adsorbed layer. However, in order to determine the thickness in the inhomogenous case, we must know how the layer is built up. For this we take advantage of the following model of the adsorbed layer: (i) The hydrocarbon portions of the surfactant molecules are associated into aggregates which include very little water. This region is indicated by HC in Figure 9. (ii) An EO–water layer surrounds the HC region, and this region is treated as a homogeneous layer with a characteristic refractive index that depends on the composition of the layer. This area is indicated as EO–water in Figure 9. (There is no need for the two EO–W regions to be equally thick or have the same composition). (iii) The concentration of EO outside the EO–W volume is negligible.

The optical properties of such a film, which may be studied by ellipsometry, can be evaluated in terms of an optical two-layer model of the adsorbed layer. This includes a HC + EO–W layer with a thickness d_{HC} and a EO–W layer with thickness $d-d_{HC}$. The refractive index of such a layer can then be evaluated by different effective-medium expressions (cf. refs 28, 29). For our system, where the difference between the refractive indices of the pure components is small, <10%, a satisfactory estimate

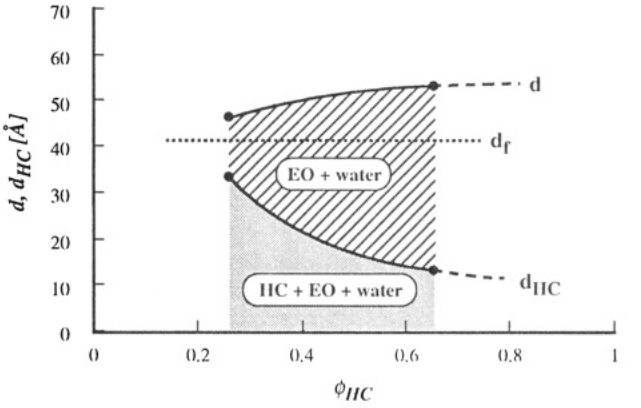

Figure 10. Possible values of the adsorbed layer thickness (d) and hydrocarbon layer thickness (d_{HC}) as a function of volume fraction (ϕ_{HC}) calculated on the basis of the optical model presented in Figure 9 from plateau adsorption data for $C_{12}E_6$. The points on the left and right hand side of the solid lines represent two extremes. The former shows the thicknesses obtained if the adsorbed layer is built up by spherical micelles with a radius corresponding to the length of fully stretched hydrocarbon chains, while the points on the right hand side represent those obtained if the hydrocarbon layer thickness is minimal and equal to that seen in the lamellar phase.[26] All thicknesses between these two extremes are possible. The dotted lines show how far this region extends if the coverage is limited by the maximal length of two extended hexaethylene oxide chains.

is obtained using the Lorentz–Lorenz relation

$$\hat{R}_{eff} = \sum_i \phi_i \hat{R}_i \tag{4}$$

where

$$\hat{R}_i = \frac{n_i^2 - 1}{n_i^2 + 2} \tag{5}$$

The variables ϕ_i and n_i are the volume fraction and the refractive index of component i, respectively. If these relations are applied to the model of the adsorbed layer, the following relations for the refractive index of the two layers are obtained

$$\hat{R}_{EO-W} = \hat{R}_{EO}\phi_{EO} + \hat{R}_W(1 - \phi_{EO}) \tag{6}$$

$$\hat{R}_{HC+EO-W} = \hat{R}_{HC}\phi_{HC} + \hat{R}_{EO-W}(1 - \phi_{HC}) \tag{7}$$

where ϕ_{EO} is the volume fraction of EO in the EO–W layer and ϕ_{HC} the volume fraction of HC in the HC + EO–W layer. ϕ_{EO} can also be expressed as

$$\phi_{EO} = \frac{V_{EO}}{V_{HC}} \frac{d_{HC}\phi_{HC}}{d - d_{HC}\phi_{HC}} \tag{8}$$

where V_{EO}/V_{HC} is the volume ratio between the ethylene oxide and hydrocarbon parts of the surfactant. The optical properties of the film can thus be described in terms of d, d_{HC}, and ϕ_{HC}. Two of these values can be determined from ellipsometer data if the third is known.

We have plotted d_{HC} and d for $C_{12}E_6$ as a function of the coverage ϕ_{HC} in Figure 10. The points indicated at the lowest coverage, ϕ_{HC} = 26%, correspond to a situation where the layer is built up by spherical micelles with a radius corresponding to the length of fully extended hydrocarbon chains, while the points at the highest coverage, ϕ_{HC} = 66%, represent the values obtained if the adsorbed layer is built up by lamellae with the smallest

(27) Tanford, C. *The Hydrophobic Effect*; Wiley: New York, 1980.
(28) Bötcher, C. J. F. *Theory of Electric Polarization*; Elsevier: Amsterdam, 1978; Vols. I, II.
(29) Looyenga, H. *Physica* **1965**, *31*, 401.
(30) Chiu, Y. C.; Chen, L. J. *Colloids Surf.* **1989**, *41*, 239.
(31) Mukerjee, P.; Mysels, K. J. *Critical Micelle Concentration*; Nat. Stand. Ref. Data Ser.; Nat. Bur. Stand. (U.S.): Washington, D.C., 1971.

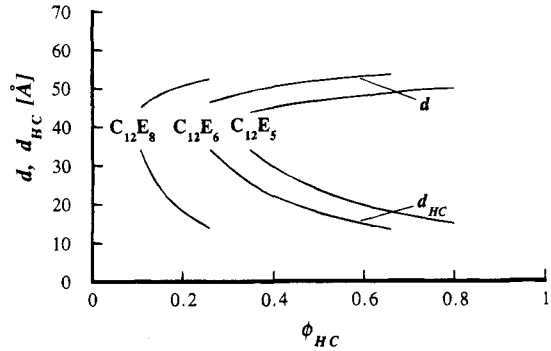

Figure 11. Possible values of the adsorbed layer thickness (d) and hydrocarbon layer thickness (d_{HC}) as a function of volume fraction (ϕ_{HC}) calculated from plateau adsorption data for dodecyl surfactants with varying lengths of the poly(ethylene oxide) chain.

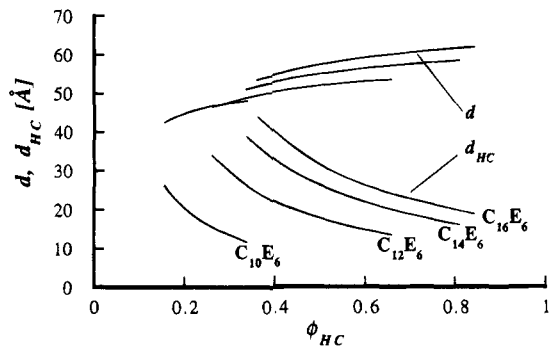

Figure 12. Possible values of the adsorbed layer thickness (d) and hydrocarbon layer thickness (d_{HC}) as a function of volume fraction (ϕ_{HC}) calculated from plateau adsorption data for hexa(ethylene glycol) surfactants with varying lengths of the hydrocarbon tail.

d_{HC} observed in the bulk lamellar phase.[26] All degrees of coverage between these extremes are possible. Values of d_{HC} and d for all surfactants studied in this region are presented in Figures 11 and 12. The thickness, d, is always larger than the optical average film thickness d_f. The reason for this is the relatively low refractive index of the EO–W layer, due to the presence of substantial amounts of water, which gives this part of the film low weight in the calculation of d_f.

The idea of an adsorbed layer built up as a complete bilayer is clearly incompatible with data for all the surfactants presented in Figures 11 and 12, but it is still not possible to evaluate the dimensions of the adsorbed surfactant aggregates without making further assumptions.

If the HC domains are viewed as pancakes (oblates), where the distance between two pancakes is twice the maximal length of the ethylene oxide chain, we can estimate the maximal axial ratio possible for the adsorbed aggregates (ϱ_{max}) as

$$\varrho_{max} = \frac{2b}{d_{HC}} \tag{9}$$

where the radius of the hydrocarbon core (b) is

$$b = \frac{d - d_{HC}}{2\left(\frac{1}{\sqrt{\phi_{HC}}} - 1\right)} \tag{10}$$

Values of ϱ_{max} for all the surfactants studied in this work are presented in Table 1. We note that the information deduced about the surfactant self-assembly structures at the silica–water interface parallels that of bulk surfactant–water systems closely. The lipophilic surfactants, $C_{12}E_5$, $C_{14}E_6$, and $C_{16}E_6$, form large surface aggregates, while the hydrophilic ones, $C_{12}E_8$ and $C_{10}E_6$, adsorb as small, possibly close to spherical, micelles. The $C_{12}E_6$ surfactant is intermediate and shows moderate micelle growth. The interaction between the surface and the surfactant molecules is weak but we still expect the surface to induce some changes in the self-assembly structure, notably promoting disk like structures. For understanding the adsorption, detailed comparative studies of surfactant self-assembly in bulk and at interfaces should be fruitful.

Conclusion

Adsorption properties of a series of nonionic surfactants have been studied and related to the molecular structure and composition of the surfactants. The adsorption process of these substances is very cooperative. At low concentrations, adsorption remains low, but as surface aggregation is initiated at a quite distinct concentration ((≈0.6–0.9)cmc), a large increase of the adsorbed amount, as well as the thickness of the adsorbed layer, is observed. The sharp increase in these parameters then levels off and reaches stable plateau values rather quickly, and these plateau values are observed around the cmc. The rise in the adsorbed amount is generally more extended for surfactants with high EO content. Mixing of two monodisperse surfactants was found to result in changes of the adsorbed layer properties that are correlated with the changes in monomer activity in bulk solution calculated by simple ideal solution theory. Slight deviations, probably due to the architectural constraints in the two-dimensional surface aggregates, were however noticed. The increase in the adsorbed layer thickness is more or less steplike for all surfactants, indicating that aggregates with a well-defined extension normal to the surface are formed prior to the cmc. Varying the number of EO groups in the surfactant does not alter the mean ellipsometrical thickness significantly, but increasing the number of hydrocarbons on the chain results in a close to linear increase of the thickness. Modeling the adsorbed layer as heterogeneous, composed of a hydrocarbon region surrounded by ethylene oxide and water, results in a slightly more complex picture. The layer thickness with this optical model is notably higher than the value of the mean optical thickness. We also conclude that all surfactants adsorb to the surface as discrete aggregates, with a size that increases with increasing hydrocarbon content.

Acknowledgment. We have benefited from stimulating discussions with Martin Hellsten, Håkan Wennerström, and Ulf Olsson. This work was sponsored by the Swedish National Board for Technical Development (NUTEK), the Swedish National Science Research Council (NFR), and the Royal Swedish Academy of Engineering Science (IVA).